Available online at www.sciencedirect.com

ScienceDirect

Journal of the European Ceramic Society 31 (2011) 1965–1973

www.elsevier.com/locate/jeurceramsoc

Sintering behaviour of celsian based ceramics obtained from the thermal conversion of (Ba, Sr)-exchanged zeolite A

A. Marocco[a], B. Liguori[b], G. Dell'Agli[a], M. Pansini[a,*]

[a] *Laboratorio Materiali, Dipartimento di Meccanica, Strutture, Ambiente e Territorio, Università di Cassino, Via Di Biasio 43, 03043 Cassino (Fr), Italy*
[b] *Dipartimento di Ingegneria dei Materiali e della Produzione, Università di Napoli "Federico II", Piazzale Tecchio 80, 80125 Napoli, Italy*

Received 11 February 2011; received in revised form 6 April 2011; accepted 17 April 2011
Available online 19 May 2011

Abstract

Five different samples of (Ba, Sr)-exchanged zeolite A, exhibiting the same Na residual content within the experimental error, were prepared by cation exchange. These powders, with or without a previous thermal treatment, were cold pressed in an isostatic press to manufacture cylindrical compacts. Such compacts were subjected to various thermal cycles up to 1500 °C. The sintering and densification of these compacts was studied by determining linear shrinkages, mass variation, bulk density and porosity. All the compacts produced were totally composed by $BaAl_2Si_2O_8$–$SrAl_2Si_2O_8$ solid solutions occurring in the polymorph known as monoclinic celsian. Porosity lower than 0.1% and bulk density higher than 95% theoretical density were obtained. The problems arising in the sintering of compacts manufactured with zeolitic precursor are discussed and proper measures to solve them are suggested.

Keywords: Sintering; Porosity; Silicate; Refractories; Monoclinic celsian

1. Introduction

Barium feldspar ($BaAl_2Si_2O_8$) and strontium feldspar ($SrAl_2Si_2O_8$) exhibit a very similar polymorphism[1-7] and their monoclinic polymorphs are materials of great technological interest on account of their excellent thermal and electrical properties. In particular, they exhibit high melting points, very good phase stability, low thermal expansion coefficient (2.52×10^{-6} and 2.68×10^{-6} °C^{-1} between 40 and 1000 °C, respectively[2]), low and thermally stable dielectric constant (7.91–7.77 and 7.50–7.39 in the range 1–100 kHz at room temperature, respectively,[2] 6.55–7.00 and 6.16–6.77 at 35 GHz between room temperature and 1200 °C, respectively[1]) and low dissipation factor (3.36×10^{-2}–0.18×10^{-2} and 3.31×10^{-2}–0.15×10^{-2} in the range 1-100 kHz at room temperature, respectively[2], 0.8×10^{-3}–4.0×10^{-3} and 1.1×10^{-3}–5.0×10^{-3} at 35 GHz in the range room temperature–1200 °C, respectively[1]). Thus, uses of these materials as refractory, high temperature electrical insulator, or as substrate for integrated circuits have been known for a long time[1], whereas applications in aeronautic and aerospace fields as a matrix material for reinforcement with continuous ceramic fibres[8] and as electromagnetic windows and radomes[1,2] are currently being studied.

Celsian and Sr-celsian give rise to solid solutions, $(Ba, Sr)Al_2Si_2O_8$, over the whole composition range of the binary state diagram $BaAl_2Si_2O_8$–$SrAl_2Si_2O_8$.[1] These solid solutions in their monoclinic form are materials that exhibit the same or even better technological properties than the respective end members on the basis of the following features:

(1) The presence of the Sr component in the solid solution at a rate not lower than 5% inhibits the high temperature monoclinic-to-hexagonal transformation, stabilizing the monoclinic form, thus increasing the service temperature of celsian-based refractories.[1]
(2) The bending strength of the monoclinic $(Ba, Sr)Al_2Si_2O_8$ solid solutions, containing more than 40% of the Ba component, is larger than that of the end members (103 and 87 MPa for $BaAl_2Si_2O_8$ and $SrAl_2Si_2O_8$, respectively), attaining a maximum of about 125 MPa for the solid solution bearing 75% of the Ba component.[1]

---

* Corresponding author.
E-mail address: pansini@unicas.it (M. Pansini).

0955-2219/$ – see front matter © 2011 Elsevier Ltd. All rights reserved.
doi:10.1016/j.jeurceramsoc.2011.04.028

(3) The monoclinic (Ba, Sr)$Al_2Si_2O_8$ solid solutions exhibit dielectric constant and dissipation factor monotonically varying between those of the celsian and Sr-celsian end members.[1]

In a previous paper[9] the thermal transformations of samples of (Ba, Sr)-exchanged zeolite A, with Sr equivalent fraction ranging from 0.14 to 0.78 and Na residual content 0.20 meq/g within the limit of experimental error, were thoroughly studied. The most interesting result of this work was that the total conversion of these samples into the monoclinic polymorph of $BaAl_2Si_2O_8$–$SrAl_2Si_2O_8$ solid solution was obtained through a 5 h thermal treatment at 1100 °C.

The results reported in Ref. [9] appear a real advance with respect to the state of the art. Actually in previous studies[10–20] it was shown that:

(1) The traditional synthesis of monoclinic celsian required prolonged heating (more than 20 h) at temperatures higher than 1500 °C.

(2) The thermal transformations of Ba-exchanged zeolite A in monoclinic celsian were strongly affected by the residual Na content of zeolite A and that the total conversion of a Ba-exchanged zeolite A sample bearing no Sr into monoclinic celsian was attained after a 22 h thermal treatment at 1300 °C, Na residual content being equal within the limit of experimental error (about 0.2 meq/g).

Thus, the presence of an amount of Sr such that $x_{Sr} = 0.14$ was sufficient to decrease the temperature and duration time of thermal treatment necessary to obtain the full conversion into the monoclinic polymorph from 1300 to 1100 °C and from 22 to 5 h, respectively.

Even the sintering ability of the monoclinic celsian obtained through the thermal transformation of Ba-exchanged zeolite A were previously investigated.[21] The results of this investigation did not appear extremely positive. Actually the values of open porosity of the full monoclinic celsian bodies obtained firing at 1300 °C for 5 h compacts manufactured uniaxially cold pressing the Ba-exchanged zeolite A powders, were slightly higher than 50%.[21] Such sintering difficulty was confirmed by Talmy et al.[1] who reported that thermal treatment at 1580 and 1550 °C were necessary to obtain a satisfactory densification of celsian and Sr-celsian, respectively, obtained by traditional method of synthesis. Nevertheless, the same authors[1] reported that monoclinic polymorph of (Ba, Sr)$Al_2Si_2O_8$ solid solutions exhibit a better sinterability than the end members of the solid solutions, demonstrated by the lower temperatures (around 1500 °C), which were necessary to attain full densification.

The previous considerations suggested that the study of the sintering ability of $BaAl_2Si_2O_8$–$SrAl_2Si_2O_8$ solid solutions obtained through the thermal transformation of (Ba, Sr)-exchanged zeolite A could be of large technological interest. Actually the presence of moderate amounts of Sr into the framework of (Ba, Sr)-exchanged zeolite A appears likely to improve the sintering ability of powders used to manufacture the green compacts without sensibly affecting the good technological properties of the monoclinic polymorph of pure $BaAl_2Si_2O_8$.

Thus, this work intends to study the sintering behaviour of $BaAl_2Si_2O_8$–$SrAl_2Si_2O_8$ solid solutions obtained through the thermal transformation of (Ba, Sr)-exchanged zeolite A. To fulfil this goal five samples of (Ba, Sr)-exchanged samples of zeolite A, having different Sr equivalent fraction (x_{Sr}), were prepared by cation exchange. These powders were used to manufacture cylindrical compacts which were subjected to various thermal cycles.

2. Experimental

Five (Ba, Sr)-exchanged zeolite A samples were prepared. The parent material, having a chemical formula of $Na_{12}Al_{12}Si_{12}O_{48}\cdot 27H_2O$ and a calculated cation exchange capacity of 5.48 meq g^{-1}, was a Carlo Erba reagent grade chemical (commercial name: zeolite 4A). The experimental cation exchange capacity of this sample of zeolite A was determined through the “batch exchange method”[22] and was not found to sensibly differ from the calculated cation exchange capacity.

Suitable samples of this material were subjected to cation exchange with $Ba(NO_3)_2$ and $Sr(NO_3)_2$ solutions, prepared by dissolving Carlo Erba reagent grade compounds in doubly distilled water (initial pH ranging between 5.8 and 6.3). The desired compositions of the five (Ba, Sr)-exchanged samples were obtained by successive approximations. Accordingly, zeolite A in its original Na form was contacted at room temperature for about 6 h with a suitable exchange solution at a solid-to-liquid ratio of 1/20 (w/w). The solid was then separated from the liquid through filtration and analyzed to establish the conditions of the following contact with a fresh exchange solution. This procedure was repeated until reaching the programmed composition of each solid. The pH of the suspensions zeolite A-solutions ranged between 6.9 and 7.0. Operative exchange conditions to obtain the five (Ba, Sr)-exchanged zeolite A samples are summarized in Table 1.

The exchanged solids, after careful washing with doubly distilled water and drying at 60 °C for 24 h, were stored at room

Table 1
Cation exchange protocol for the preparation of the (Ba, Sr)-rich zeolite A samples.

Sample no.	Exchange cycles	Exchange solution	
		$[Sr^{2+}]$, M	$[Ba^{2+}]$, M
1	1st	0.20	0.20
	2nd–8th	0.01	0.10
2	1st–5th	no	0.10
	6th–8th	0.02	no
3	1st–5th	no	0.10
	6th–7th	0.05	no
4	1st–2nd	0.07	no
	3th–5th	no	0.10
	6th	0.07	0.10
	7th	0.07	no
5	1st–6th	0.10	no
	7th–11th	no	0.01
	12th	no	0.10

Table 2
Cation composition of (Ba, Sr)-exchanged zeolite A samples.[a]

Sample	No. (Table 1)	[Na] meq g^{-1}	x_{Na}	x_{Ba}	x_{Sr}	$x_{Sr}/(x_{Ba}+x_{Sr})$
$Ba_{0.83}$,$Sr_{0.14}$-A	1	0.18	0.03	0.83	0.14	0.19
$Ba_{0.74}$,$Sr_{0.22}$-A	2	0.23	0.04	0.74	0.22	0.27
$Ba_{0.56}$,$Sr_{0.41}$-A	3	0.14	0.03	0.56	0.41	0.42
$Ba_{0.48}$,$Sr_{0.49}$-A	4	0.18	0.03	0.48	0.49	0.51
$Ba_{0.19}$,$Sr_{0.78}$-A	5	0.16	0.03	0.19	0.78	0.80

[a] [Na] = residual, unexchanged Na content; x_{Na}, x_{Ba}, x_{Sr} = Na, Ba and Sr equivalent fractions.

temperature over saturated $Ca(NO_3)_2$ solution (relative humidity near 50%).

Solids were analyzed according to the following procedure. After calcination, a weighted amount of the dry samples was subjected to digestion, under microwave-induced heating (Perkin-Elmer Multiwave 3000 oven), in a standard solution prepared by mixing 1 ml of HCl (37%, w/w), 1 ml of HNO_3 (65%, w/w) and 4 ml of HF (39.5%, w/w). After addition of 24 ml of a 8 M H_3BO_3 solution to attain fluoride complexation, the resulting solution was analyzed by ICP-OES, using a Perkin-Elmer Optima 2100 DV ICP-OES apparatus.

Table 2 reports the cation composition of the five (Ba, Sr)-A samples, which are labelled, and will be identified from this point onwards, as Ba_xSr_y-A, where x and y are the equivalent fractions of the two extraframework cations, made 1 the sum of the total exchangeable cations. Note that, as a rule, $x + y < 1$, considering that some minor Na^+ remained in the various samples at the end of the exchange operations. The residual Na^+ content, ranging between 0.14 and 0.23 meq g^{-1}, which appears not further exchangeable, involves the possible presence of some $NaAlO_2$ occluded in the β-cages of the zeolite framework, as frequently reported by literature.[23,24] It must be noticed that the differences recorded in the residual Na content of various samples appear within the experimental error which means that, in practice, the various samples exhibit the same residual Na content.

The powders obtained as previously described, were subjected to room temperature X-ray diffraction (XRD) using a Philips X'PERT diffractometer, Cu Kα radiation, collection of data for 2θ varying between 10° and 60° with a step width 2θ equal to 0.02° and 1 s data collection per step. Moreover their grain size distribution was determined using an Analysette 22 Fritsch laser particle sizer.

Cylindrical compacts, having diameter $d = 25$ mm and height $h = 5$ mm, were manufactured by putting the due amount of these powders in cylindrical moulds and by pressing them at 150 MPa with an isostatic press (ABB, CIP 32330-P2 model). It must be said that in some case the original powders with no previous thermal treatment were used, and in some other case the original powders were thermally treated in various ways before manufacturing the compacts. Such compacts were, in their turn, subjected to different thermal cycles in order to attain the best sintering conditions. For all thermal treatments a Lenton furnace, which ensures stable temperature to within ±2 °C, and platinum crucibles were used. The different modalities through which the compacts were manufactured and the various thermal treatments to which the compacts themselves were subjected, are grouped in cycles and are described in detail hereafter.

Cycle 1 – The compacts were manufactured with original powders of samples $Ba_{0.83}$,$Sr_{0.14}$-A and $Ba_{0.56}$,$Sr_{0.41}$-A with no previous thermal treatment. These compacts were heated at 5 °C/min heating rate in the temperature range room temperature–500 °C and at 10 °C/min heating rate in the temperature range 500–1300 °C, kept at 1300 °C for 5 h, cooled at 20 °C/min cooling rate in the temperature range 1300–800 °C. Subsequently the furnace was switched off and the compacts left inside until they cooled down to room temperature.

Cycle 2 – The compacts were manufactured with original powders of samples $Ba_{0.83}$,$Sr_{0.14}$-A and $Ba_{0.56}$,$Sr_{0.41}$-A with no previous thermal treatment. These compacts were heated at 5 °C/min heating rate in the temperature range room temperature–500 °C and at 10 °C/min heating rate in the temperature range 500–1400 °C, kept at 1400 °C for 5 h, cooled at 20 °C/min cooling rate in the temperature range 1400–800 °C. Subsequently the furnace was switched off and the compacts left inside until they cooled down to room temperature.

Cycle 3 – The compacts were manufactured with original powders of samples $Ba_{0.83}$,$Sr_{0.14}$-A and $Ba_{0.56}$,$Sr_{0.41}$-A with no previous thermal treatment. These compacts were heated at 1 °C/min heating rate in the temperature range room temperature–1400 °C and kept at 1400 °C for 5 h. Subsequently the furnace was switched off and the compacts left inside until they cooled down to room temperature. In the bottom of the platinum crucibles in which the thermal treatment of the compact was performed, the due amount of the same powder used to manufacture the green compact was previously deposited in order to create a powder bed where to lay the green compact itself before firing. This same expedient was used also in cycles 4–9.

Cycle 4 – The compacts were manufactured with original powders of samples $Ba_{0.83}$,$Sr_{0.14}$-A and $Ba_{0.56}$,$Sr_{0.41}$-A with no previous thermal treatment. These compacts were heated at 1 °C/min heating rate in the temperature range room temperature–1500 °C and kept at 1500 °C for 5 h. Subsequently the furnace was switched off and the compacts left inside until they cooled down to room temperature. The compacts were laid in a powder bed (see cycle 3).

Cycle 5 – The powders of sample $Ba_{0.83}$,$Sr_{0.14}$-A and $Ba_{0.56}$,$Sr_{0.41}$-A were heated at 10 °C/min heating rate up to 200 °C and kept at this temperature for 2 h. Subsequently the furnace was switched off and the powders left inside until they cooled down to room temperature. The compacts manufactured with these powders were heated at 1 °C/min heating rate in the temperature range room temperature–1500 °C and kept at 1500 °C for 5 h. Subsequently the furnace was switched off and the compacts left inside until they cooled down to room temperature. The compacts were laid in a powder bed (see cycle 3).

Cycle 6 – The powders of sample $Ba_{0.83}$,$Sr_{0.14}$-A and $Ba_{0.56}$,$Sr_{0.41}$-A were heated at 10 °C/min heating rate up to 200 °C and kept at this temperature for 2 h. Subsequently the furnace was switched off and the powders left inside until they cooled down to room temperature. The compacts manufactured with these powders were heated at 1 °C/min heating rate in the temperature range room temperature–1500 °C, kept at 1500 °C for 5 h, cooled at 1 °C/min cooling rate in the temperature range 1500–800 °C. Subsequently the furnace was switched off and the compacts left inside until they cooled down to room temperature. The compacts were laid in a powder bed (see cycle 3).

Cycle 7 – The powders of sample Ba$_{0.83}$,Sr$_{0.14}$-A and Ba$_{0.56}$,Sr$_{0.41}$-A were heated at 10 °C/min heating rate up to 500 °C and kept at this temperature for 2 h. Subsequently the furnace was switched off and the powders left inside until they cooled down to room temperature. The compacts manufactured with these powders were heated at 1 °C/min heating rate in the temperature range room temperature–1500 °C and kept at 1500 °C for 5 h. Subsequently the furnace was switched off and the compacts left inside until they cooled down to room temperature. The compacts were laid in a powder bed (see cycle 3).

Cycle 8 – The powders of sample Ba$_{0.83}$,Sr$_{0.14}$-A, Ba$_{0.56}$,Sr$_{0.41}$-A and Ba$_{0.48}$,Sr$_{0.49}$-A were heated at 10 °C/min heating rate up to 1200 °C and kept at this temperature for 5 h. Subsequently the furnace was switched off and the powders left inside until they cooled down to room temperature. Such powders were mixed with 10 wt% original thermally untreated powders of the same sample Ba$_{0.83}$,Sr$_{0.14}$-A, Ba$_{0.56}$,Sr$_{0.41}$-A and Ba$_{0.48}$,Sr$_{0.49}$-A, respectively. The compacts manufactured with these mixed powders were heated at 1 °C/min heating rate in the temperature range room temperature–1500 °C, kept at 1500 °C for 5 h, cooled at 1 °C/min cooling rate in the temperature range 1500–700 °C. Subsequently the furnace was switched off and the compacts left inside until they cooled down to room temperature. The compacts were laid in a powder bed (see cycle 3).

Cycle 9 – The powders of sample Ba$_{0.83}$,Sr$_{0.14}$-A, Ba$_{0.74}$,Sr$_{0.22}$-A, Ba$_{0.56}$,Sr$_{0.41}$-A, Ba$_{0.48}$,Sr$_{0.49}$-A and Ba$_{0.19}$,Sr$_{0.78}$-A were heated at 10 °C/min heating rate up to 1200 °C and kept at this temperature for 5 h. Subsequently the furnace was switched off and the powders left inside until they cooled down to room temperature. These powders were added with different amounts of doubly distilled water. In particular sample Ba$_{0.83}$,Sr$_{0.14}$-A was added with 4, 5 and 6 wt%, sample Ba$_{0.74}$,Sr$_{0.22}$-A with 5 wt%, sample Ba$_{0.56}$,Sr$_{0.41}$-A with 5 and 6 wt%, sample Ba$_{0.48}$,Sr$_{0.49}$-A with 5 and 6 wt% and sample Ba$_{0.19}$,Sr$_{0.78}$-A with 5 wt.% doubly distilled water. The compacts, manufactured with these powders and added with doubly distilled, water were heated at 1 °C/min heating rate in the temperature range room temperature–1500 °C, kept at 1500 °C for 5 h, cooled at 1 °C/min cooling rate in the temperature range 1500–700 °C. Subsequently the furnace was switched off and the compacts left inside until they cooled down to room temperature. The compacts were laid in a powder bed (see cycle 3).

The most meaningful part of the products of the thermal cycles previously described was characterized as follows:

(1) By room temperature X-ray diffraction using the same Philips 1730 X-ray diffractometer previously described.
(2) By determining the weight loss and linear shrinkage.
(3) By determining the porosity according to ASTM C373-88 (2006) regulation.[25] This regulation recommends to measure the weight of the fired product in air (W_1), the weight of the water saturated fired product immersed in water (W_2) and the weight of the water saturated fired product in air (W_3). If V is the geometric volume of the fired product and the specific gravity of water is considered equal to unity, the following quantities may be defined:
    geometric volume $V = W_3 - W_2$
    bulk density, $d_b = W_1/V$
    apparent density, $d_a = W_1/(W_1 - W_2)$
    percent porosity, $p = (W_3 - W_1)\ 100/V$
(4) By scanning electron microscopy using a Philips XL30 apparatus. In some case the compacts were etched for 15 s in a 0.5% hydrofluoric acid aqueous solution before performing the micrograph. This etching procedure results in a mild chemical attack to grain borders which allow to evidence the dimension of grains of crystalline phases present in the compact.

3. Results

Fig. 1 reports the grain size distribution curve of sample Ba$_{0.83}$, Sr$_{0.14}$-A, which is very similar to those of other samples (not reported). The main features of this particle size distribution curve, which appears essentially monomodal are the following: (1) The average diameter of particles is about 10–12 µm; (2) About 90 wt.% exhibits grain size lower than about 21 µm; (3) About 5 wt.% exhibits grain size lower than 1 µm; (4) About 90 wt.% exhibits grain size ranging between 5 and 24 µm.

XRD patterns of powders obtained crushing some of the compacts produced in all the cycles were performed. All such patterns, which closely resemble to each other, revealed that all the considered powders were totally composed by the monoclinic polymorph of $\mathrm{BaAl_2Si_2O_8}$–$\mathrm{SrAl_2Si_2O_8}$ solid solution (JCPDS card n. 38–1450) in perfect agreement with Ref. [2]. As an example, Fig. 2 reports the XRD pattern of the powder obtained crushing the compact manufactured with sample Ba$_{0.83}$,Sr$_{0.14}$-A and 5 wt.% doubly distilled water according to what reported in cycle 9.

The main results of the characterization performed on the compacts manufactured according to what reported in experimental, are summarised in Table 3. The quantities reported in this table are: the percent mass variation (Δm %), the percent linear shrinkage (Δd %), the bulk density (d_b, g/cm^3),

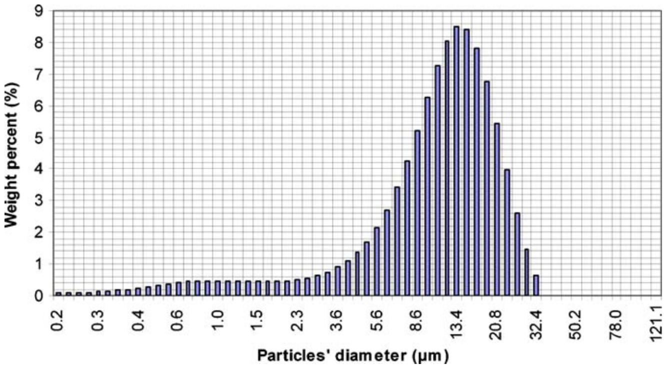

Fig. 1. Grain size distribution curve of sample Ba$_{0.83}$,Sr$_{0.14}$-A.

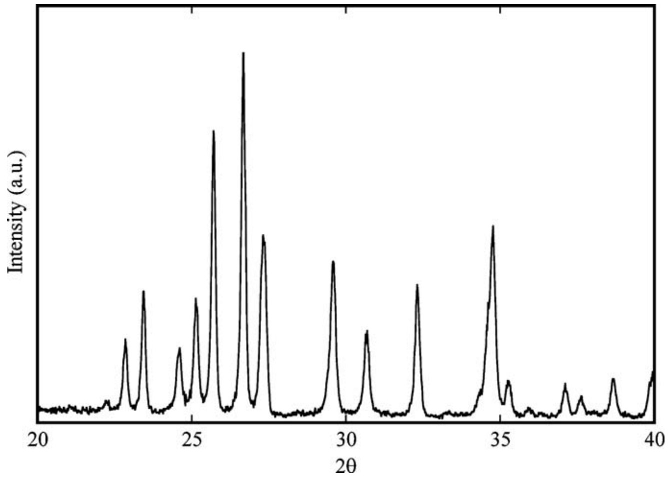

Fig. 2. XRD pattern of the powder obtained crushing the compact manufactured with sample $Ba_{0.83}$,$Sr_{0.14}$-A and 5 wt.% doubly distilled water according to cycle 9.

Table 3
Percent mass variation (Δ*m* %), percent linear shrinkage (Δ*d* %), bulk density (d_b, g/cm^3), percent porosity (*p* %) and (bulk density)/(theoretical density) percent ratio (d_b/d_t %).

Sample	Δ*m* %	Δ*d* %	d_b, g/cm^3	*p* %	d_b/d_t %
Cycle 1					
$Ba_{0.83}$,$Sr_{0.14}$-A	18.2	18.0	2.38	27.0	71.3
$Ba_{0.56}$,$Sr_{0.41}$-A	21.4	21.8	2.62	16.5	80.4
Cycle 2					
$Ba_{0.83}$,$Sr_{0.14}$-A	21.2	21.2	2.70	16.3	80.8
$Ba_{0.56}$,$Sr_{0.41}$-A	21.7	23.6	2.80	10.8	85.9
Cycle 3					
$Ba_{0.83}$,$Sr_{0.14}$-A	19.1	21.8	2.71	16.6	81.1
$Ba_{0.56}$,$Sr_{0.41}$-A	20.1	23.0	2.76	13.7	84.7
Cycle 4					
$Ba_{0.83}$,$Sr_{0.14}$-A	19.4	23.0	3.10	0.6	92.8
$Ba_{0.56}$,$Sr_{0.41}$-A	20.9	24.0	3.02	0.8	92.6
Cycle 5					
$Ba_{0.83}$,$Sr_{0.14}$-A	9.6	21.0	3.09	1.1	92.5
$Ba_{0.56}$,$Sr_{0.41}$-A	10.2	21.3	3.00	1.2	92.0
Cycle 6					
$Ba_{0.83}$,$Sr_{0.14}$-A	11.4	21.8	3.13	<0.1	93.7
$Ba_{0.56}$,$Sr_{0.41}$-A	11.7	22.2	3.03	0.4	92.9
Cycle 7					
$Ba_{0.83}$,$Sr_{0.14}$-A	2.1	17.6	3.15	0.5	94.3
$Ba_{0.56}$,$Sr_{0.41}$-A	1.7	17.4	2.98	2.0	91.4
Cycle 8					
$Ba_{0.83}$,$Sr_{0.14}$-A	2.4	15.4	3.13	1.2	93.7
$Ba_{0.56}$,$Sr_{0.41}$-A	2.3	16.3	2.99	2.4	91.7
$Ba_{0.48}$,$Sr_{0.49}$-A	2.4	15.6	3.03	1.2	93.5
Cycle 9					
$Ba_{0.83}$,$Sr_{0.14}$-A (4% H_2O)	0.4	16.3	3.13	<0.1	93.7
$Ba_{0.83}$,$Sr_{0.14}$-A (5% H_2O)	0.6	12.5	3.18	<0.1	95.2
$Ba_{0.83}$,$Sr_{0.14}$-A (6% H_2O)	0.1	14.7	3.16	<0.1	94.6
$Ba_{0.74}$,$Sr_{0.22}$-A (5%H_2O)	0.3	14.7	3,16	<0.1	95.2
$Ba_{0.56}$,$Sr_{0.41}$-A (5% H_2O)	0.2	14.0	3.10	<0.1	95.1
$Ba_{0.56}$,$Sr_{0.41}$-A (6% H_2O)	0.2	13.7	3.05	<0.1	93.6
$Ba_{0.48}$,$Sr_{0.49}$-A (5% H_2O)	0.6	14.8	3.08	<0.1	95.1
$Ba_{0.48}$,$Sr_{0.49}$-A (6% H_2O)	0.2	15.2	3.02	<0.1	93.2
$Ba_{0.19}$,$Sr_{0.78}$-A (5%H_2O)	0.3	13.6	2.92	<0.1	92.9

the percent porosity (*p* %) and the (bulk density)/(theoretical density) percent ratio (d_b/d_t %). The value of the theoretical density d_t, to which the bulk density d_b of the compacts was referred, was the value of the theoretical density of the monoclinic polymorph of $BaAl_2Si_2O_8$–$SrAl_2Si_2O_8$ solid solution. Such theoretical density values were computed performing a linear interpolation based on the equivalent fraction of Ba and Sr between the value of the theoretical density of pure monoclinic polymorph of $BaAl_2Si_2O_8$ (3.39 g/cm^3,[26]) and the value of the theoretical density of pure monoclinic polymorph of $SrAl_2Si_2O_8$ (3.08 g/cm^3,[27]). Thus the values of the theoretical density of sample $Ba_{0.83}$,$Sr_{0.14}$-A, $Ba_{0.74}$,$Sr_{0.22}$-A, $Ba_{0.56}$,$Sr_{0.41}$-A, $Ba_{0.48}$,$Sr_{0.49}$-A and $Ba_{0.19}$,$Sr_{0.78}$-A turned out 3.34, 3.32, 3.26, 3.24 and 3.14 g/cm^3, respectively.

In commenting these data it must be said that the compacts thermally treated according to cycles 1 and 2 presented more or less evident fractures, which did not occur in the compacts thermally treated according to the remaining cycles. The most striking features of data reported in Table 3 are summarised hereafter:

(1) Compacts manufactured with thermally untreated powders (cycles 1–4) exhibit high (about 20%) mass variation and linear shrinkage.
(2) Compacts manufactured with powders which were previously thermally treated at 200 °C for 2 h (cycles 5 and 6), exhibit similar linear shrinkage (about 20%) and lower mass variation (about 10%).
(3) Raising the temperature and the duration time of the thermal treatment to which the powders were subjected before manufacturing the green compacts results in lower mass variation (about 2% for thermal treatment at 500 °C, cycle 7, and up to 0.1% for thermal treatment at 1200 °C, cycle 9) and linear shrinkage (about 17% for thermal treatment at 500 °C, cycle 7, and from 12 to 16% for thermal treatment at 1200 °C, cycles 8 and 9).
(4) A slow heating rate (1 °C/min) and the use of the powder bed described in experimental avoided the occurrence of fractures in the compacts.
(5) Raising the temperature and the duration time of the thermal treatment to which the powders were subjected before manufacturing the green compacts results in increasing bulk density and decreasing percent porosity of compacts.
(6) Raising the temperature of the thermal treatment to which the green compacts were fired results in increasing bulk density and decreasing percent porosity of compacts. In particular bulk density ranging between 92.9 and 95.2% of theoretical density and porosity decidedly lower than 0.1% were recorded in the compacts manufactured according to cycle 9.
(7) No significant differences of mass variation, linear shrinkage, bulk density and porosity were recorded in the compacts manufactured with powder bearing different amounts of Ba and Sr.

SEM micrographs of compacts thermally treated according to cycle 9 were performed. In agreement with data of Table 3,

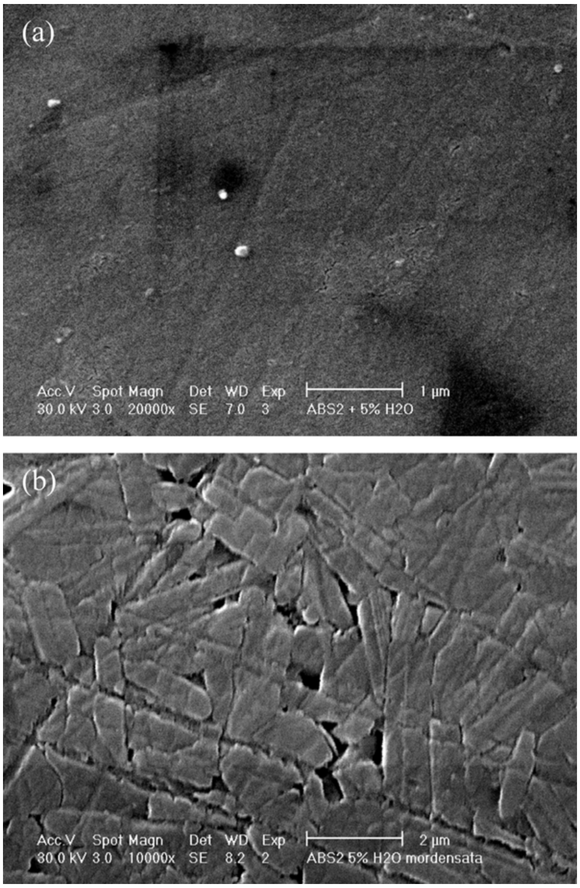

Fig. 3. SEM micrograph of the compact manufactured with sample $Ba_{0.83}$,$Sr_{0.14}$-A and 5 wt.% doubly distilled water according to cycle 9. Part a: original compact with no etching procedure, part b: compact etched for 15 s in a 0.5% hydrofluoric acid aqueous solution.

such micrographs, which appear quite similar to each other, evidence products exhibiting good compactness. In particular Fig. 3 reports the SEM micrograph of the compacts manufactured with the powder of sample $Ba_{0.83}$,$Sr_{0.14}$-A, previously thermally treated for 5 h at 1200 °C, added with 5% doubly distilled water and subsequently fired at 1500 °C for 5 h. Micrograph a, performed on the original compact with no etching procedure, confirms the good compactness of the products. The etching procedure to which the compact portrayed in micrograph b was subjected, evidenced the grains of the monoclinic polymorph of $BaAl_2Si_2O_8$–$SrAl_2Si_2O_8$ solid solutions which make up the compact. The length of such grains appears to range between 1 and 2 μm.

4. Discussion

In Ref. [21] it was reported that the values of open porosity of the full monoclinic celsian bodies obtained firing at 1300 °C for 5 h compacts manufactured uniaxially cold pressing the Ba-exchanged zeolite A powders, were slightly higher than 50%. All the results reported in this work, even the most negative, appear a real advance with respect to the results of Ref. [21]. Actually even in cycle 1, in which the green compacts were fired at 1300 °C for 5 h, porosities of 16.5 and 27% were recorded. Such a large advance is, in the opinion of the authors, mainly related to the use of an isostatic press in the manufacture of the compacts. Actually it is well known that using an isostatic press in the manufacture of green compacts, rather than an uniaxial one, results in increasing the densification of the fired ceramic bodies.[28] It appears likely that such improvement may be even more marked in the case of sintering of zeolitic precursors. Actually the hydrostatic distribution of pressures created by the isostatic press seems a crucial support in overcoming the difficulties arising in the sintering of a material which exhibits an intrinsic microporosity and evolves large amounts of water upon heating such as the zeolitic precursor.

These same difficulties appear likely to result in the more or less evident fractures recorded in the compacts thermally treated according to cycles 1 and 2. Actually sintering of thermally untreated zeolitic precursor results in high mass variation and linear shrinkage (about 20%) arising from the zeolitic water evolution upon heating and thermal collapse of microporous zeolitic structure.[9] Nevertheless the occurrence of the fractures was avoided by simply slowing down heating and cooling rates and by laying the compacts in the powder bed described in experimental. It appears evident that the former expedient resulted in milder, less abrupt, volume variations, whereas the latter supplies a softer surface which better accommodates the compacts during their firing.

Several attempts were performed in order to improve the sintering and the densification of the compacts manufactured with the samples of (Ba, Sr)-exchanged zeolite A powders. In particular the temperature at which the compacts were fired, was raised from 1300 to 1400 and 1500 °C and the compacts themselves were manufactured with powders which were previously subjected to thermal treatments at 200, 500 or 1200 °C. Such measures appeared necessary to tackle the still unsatisfactory densification and the previously cited high mass variation and linear shrinkage arising from the zeolitic water evolution upon heating and thermal collapse of microporous zeolitic structure. The lone raising of the temperature at which the compacts were fired increased the densification of the compact (from about 70 up to slightly more than 90% of the theoretical density with porosity of about 0.6–0.8%) but did not sensibly reduce the mass variation and linear shrinkages. The combined raising of the temperature at which the compacts were fired and raising of the temperature at which powders were thermally treated before manufacturing the compacts resulted in a further improvement of densification (up to 95.2% of the theoretical density), in dramatic reductions of mass variations (lower than 1%) and sensible reductions of linear shrinkages (to about 12–16%).

These findings may be explained considering that (Ba, Sr)-exchanged zeolite A undergoes increasing structural damages with increasing temperature and increasing Ba content.[9] In particular it was found that thermally treating the samples used in this work at 200 and 500 °C results in a partial and in an almost total thermal collapse of the microporous zeolite structure, respectively, and that such thermal collapse goes to completion between 700 and 800 °C. On the basis of these considerations it appears evident that the lone raising of the temperature at which the compacts were fired increased the densification of the compact on account of the increased atomic mobility, whereas no reductions of mass variation and linear shrinkage may be expected from a material such as the thermally untreated (Ba, Sr)-exchanged zeolite A characterised by a microscopic porosity full of about 20 wt.% zeolitic water.[9] Thus, the dramatic reductions of mass variations and sensible reductions of linear shrinkages may be reasonably ascribed to thermal treatments to which the powders were subjected before manufacturing the compacts. As far as mass variation are concerned, their values go from about 20% (no thermal treatment) to about 10–11 wt.% (thermal treatment at 200 °C), to about 2 wt.% (thermal treatment at 500 °C), and finally to lower than 1 wt.% (thermal treatment at 1200 °C). Such variations are perfectly consistent with the thermally induced structural evolution of (Ba, Sr)-exchanged zeolite A. Actually the partially damaged microporous zeolitic structure arising from a 200 °C thermal treatment retains a part of its original zeolitic water, whereas such zeolitic water dramatically decreases upon thermal treatment of powders at 500 °C on account of the increased structural damage. Obviously the amount of water retained by the damaged zeolitic structure was evolved during the firing of the compact, thus, giving rise to the mass variation recorded.

The mass variations recorded in cycles 8 and 9 require some further consideration. The thermal treatment at 1200 °C to which the powders were subjected completely destroyed the microporous zeolite structure which brought practically to zero the amount of the zeolitic water present in the systems and promoted the thermal transformation of the system initially in the hexagonal and subsequently in the monoclinic polymorph of $BaAl_2Si_2O_8$–$SrAl_2Si_2O_8$ solid solution.[9] This finding should result in practically zero mass variations. This seeming inconsistency may be explained considering that the manufacture of compacts according to cycles 8 and 9 needed the use of a temporary binder, unlike the manufacture of the compacts according to all the remaining cycles. Actually the zeolitic water, present in sufficient amount in the powders used to manufacture the compacts of cycle 1–7, acted as temporary binder, which did not occur for compacts manufactured according to cycle 8 and 9. Thus, 10 wt.% of original thermally untreated homologous (Ba, Sr)-exchanged zeolite A and amounts of doubly distilled water ranging from 4 to 6 wt.% were used as temporary binder in cycles 8 and 9, respectively. Obviously the mass variation recorded in cycles 8 and 9 may be ascribed to the deliberately added temporary binder. Moreover reported data seem to suggest that doubly distilled water works better as temporary binder and that 5 wt.% is its optimum value.

Nevertheless all the attempts performed allowed only a sensible reduction of linear shrinkage (to about 12—16%). This finding may reasonably be ascribed to the grain size distribution curve reported in Fig. 1. Actually about 90 wt.% of the powder used to manufacture the compacts exhibits grain size ranging between 5 and 24 μm. Such a narrow grain size distribution likely results in green compacts which exhibit an high amount of voids which give rise to the recorded linear contractions on firing.

An other remark that may be done is that the different amount of Sr present in the various samples do not seem to sensibly affect the obtained results. Nevertheless in Ref. [9] the authors found that the presence of an amount of Sr such that $x_{Sr} = 0.14$ was sufficient to decrease the temperature and duration time of thermal treatment necessary to obtain the full conversion into the monoclinic polymorph from 1300 to 1100 °C and from 22 to 5 h, respectively. Thus, it appears likely that even the sintering and densification of compacts manufactured with (Ba, Sr)-exchanged zeolite A powders is facilitated and expedited by the presence of moderate Sr amounts.

The authors retain meaningful the comparison of the results of this work with those collected in Ref. [26]. The authors of this work studied the microstructural development and densification of Ba- and (Ba, Li)-exchanged zeolite X precursors. These authors reports the following data:

(1) Thermally treating for 35 h at 1550 °C green compacts manufactured by uniaxial cold pressing at 105 MPa powders of Ba-exchanged zeolite X resulted in a monoclinic celsian body exhibiting 86.8% theoretical density.
(2) Thermally treating for 6 h at 1200 °C green compacts manufactured by uniaxial cold pressing at 105 MPa powders of (Ba, Li)-exchanged zeolite X (composition: $0.11Na_2O{\cdot}0.16LiO_2{\cdot}0.72BaO{\cdot}Al_2O_3{\cdot}2.46\ SiO_2$) with 1 wt.% seeds resulted in a monoclinic celsian body exhibiting 84.5% theoretical density.
(3) Thermally treating for 2 h at 910 °C under a stress of 5.7 MPa and for 1 h at 1090 °C under the same stress green compacts manufactured by uniaxial cold pressing at 105 MPa powders of (Ba, Li)-exchanged zeolite X (composition: $0.11Na_2O{\cdot}0.16LiO_2{\cdot}0.72BaO{\cdot}Al_2O_3{\cdot}2.46\ SiO_2$) resulted in a monoclinic celsian body exhibiting 90.3% theoretical density.
(4) Thermally treating for 2 h at 880 °C under a stress of 21 MPa and for 0.5 h at 1050 °C under the same stress green compacts manufactured by uniaxial cold pressing at 105 MPa powders of (Ba, Li)-exchanged zeolite X (composition: $0.11Na_2O{\cdot}0.16LiO_2{\cdot}0.72BaO{\cdot}Al_2O_3{\cdot}2.46SiO_2$) resulted in a monoclinic celsian body exhibiting 91.1% theoretical density.

It appears noticeable that in this work densification higher by more than 4% were obtained although expensive sintering techniques such as hot pressing were not used like in Ref. [26].

5. Conclusions

The technique proposed by Subramanian and coworkers[29–32] of thermal transformations of alkaline or alkaline-earth cations exchanged zeolites into ceramics presents the main following advantages:

(1) More than 200 zeolites are known[33] and many of them exhibit Si/Al ratios continuously varying in quite extended ranges.[23] Cation exchange operations do not display any difficulty on many zeolitic terms, which allow to easily obtain different cation compositions and even to introduce in the zeolites the proper amounts of cations having mineralis-

ing action such as lithium. This allows access to a material which always exhibits the desired starting composition.

(2) The amorphous phase arising from the thermal collapse of the microporous zeolite structure exhibits a perfect homogeneity of composition, which is known to play a crucial role in attaining the best technological properties in ceramic materials.

(3) The fact that the zeolites are widely used for many industrial and technological applications drew attention of researchers towards the synthesis of the zeolitic terms used in these processes. Thus, these synthesis procedures were already optimized, resulting in low cost of the starting materials.

Nevertheless this technique presents also the following fundamental drawback: a compact manufactured with a zeolitic precursor exhibits bulk density of about 1.5 g/cm^3, [26] whereas the theoretical density of the sintered ceramic bodies should tend as much as possible to values even higher than 3 g/cm^3. [26] This work has shown that this drawback may be successfully tackled by using some simple, not expensive, expedient. Among them the use of slow heating and cooling rates, the use of the powder bed described in experimental, the use of an isostatic press in the manufacture of the green compacts, the set up of the most proper thermal cycles of treatment of powders prior to the manufacture of the green compacts and the set up of the most proper thermal cycles for the final firing of the green compacts themselves.

The results of this work seem to suggest also an other simple expedient to improve the sintering behaviour of zeolitic precursors. The moderately high linear shrinkages (13–16%) recorded in cycle 9 might hinder the use of (Ba, Sr)-exchanged zeolite A as a precursor for the synthesis of the monoclinic polymorph $BaAl_2Si_2O_8$–$SrAl_2Si_2O_8$ solid solutions. Such linear shrinkages could be largely reduced if the grain size distribution of the starting zeolite A were more favourable. Actually the grain size distribution curve of zeolite A used in this work appeared essentially monomodal inasmuch as about 90 wt.% exhibited grain size ranging between 5 and 24 μm. If the use of zeolites as raw materials for ceramics manufacture became a common practice, it would not be a great difficulty for zeolite producers to slightly modify zeolite production processes in order to obtain a larger and not monomodal grain size distribution range which could very likely facilitate the sintering and densification of the green compacts.

References

1. Talmy IG, Haught DA, Wuchina EJ. In: Goldberg AB, Harper CA, Schroeder MS, Ibraham MA, editors. *Ceramic in the system BaO. Al_2O_3·2SiO$_2$–SrO·Al_2O_3·2SiO$_2$ (BAS–SAS) polymorphism, processing and properties*. 1992. p. 687.
2. McCauley RA. Polymorphism and dielectric properties of Ba- and Sr-containing feldspars. *J Mater Sci* 2000;**35**:3939–42.
3. Yoshiki B, Matsumoto K. High temperature modification of Barium feldspar. *J Am Ceram Soc* 1951;**34**:283–6.
4. Colella C, Aiello R. Thermal conversion of synthetic cymrite into hexagonal barium feldspar. *Thermochim Acta* 1978;**27**:253–60.
5. Muller WF. Phase transitions and associated domain in hexacelsian ($BaAl_2Si_2O_8$). *Phys Chem Miner* 1977;**1**:71–82.
6. Lin HC, Foster WR. Studies in the system BaO–Al_2O_3–SiO_2, I. The polymorphism of celsian. *Am Miner* 1962;**53**:134–44.
7. Ferone C, Esposito S, Pansini M. Microwave assisted hydrothermal conversion of Ba-exchanged zeolite A into metastable paracelsian. *Micropor Mesopor Mater* 2006;**96**:9–13.
8. Bansal NP. Solid state synthesis and properties of monoclinic celsian. *J Mater Sci* 1998;**33**:4711–5.
9. Ferone C, Liguori B, Marocco A, Anaclerio S, Pansini M, Colella C. Monoclinic (Ba, Sr)-celsian by thermal treatment of (Ba, Sr)-exchanged zeolite A. *Micropor Mesopor Mater* 2010;**134**:65–71.
10. Dell'Agli G, Ferone C, Mascolo MC, Pansini M. Thermal transformation of Ba-exchanged A and X zeolites into monoclinic celsian. *Solid State Ionics* 2000;**127**:309–17.
11. Dell'Agli G, Ferone C, Mascolo MC, Pansini M. New insight into the thermal transformation of Barium-exchanged zeolite A to celsian. *Chem Mater* 2002;**14**:797–803.
12. Aronne A, Esposito S, Ferone C, Pansini M, Pernice P. FTIR study of the thermal transformation of Barium-exchanged zeolite A to celsian. *J Mater Chem* 2002;**12**:3039–45.
13. Esposito S, Ferone C, Pansini M, Bonaccorsi L, Proverbio E. A comparative study of the thermal transformations of Ba-exchanged zeolites A, X and LSX. *J Eur Ceram Soc* 2004;**24**:2689–97.
14. Clayden N, Esposito S, Ferone C, Pansini M. ^{29}Si and ^{27}Al NMR study of the thermal transformation of barium exchanged zeolite-A to celsian. *J Mater Chem* 2003;**13**:1681–5.
15. Ferone C, Esposito S, Dell'Agli G, Pansini M. Role of Li in the low temperature synthesis of monoclinic celsian from (Ba, Li)-exchanged zeolite-A precursor. *Solid State Sci* 2005;**7**:1406–14.
16. Ferone S, Esposito M, Pansini. Thermally induced structural and microstructural evolution of barium exchanged zeolite A to celsian. In: Gamba A, Colella C, Coluccia S, editors. *Oxide based materials. New sources, novel phasesm, new applications. Studies in surface science and catalysis*, 155. Amsterdam: Elsevier B.V.; 2005. p. 249–60.
17. Ferone C, Marocco A, Pansini M, Dell'Agli G, Esposito S. Effect of residual Na on the low temperature synthesis of monoclinic celsian from zeolite Ba-A. In: Gedeon A, Massiani P, Babonneau F, editors. *Zeolites and related materials: trends, targets and challenges, studies in surface science and catalysis*, vol. 174. Amsterdam: Elsevier; 2008. p. 197–200. Part I.
18. Clayden N, Esposito S, Ferone C, Pansini M. Substitution clustering in a non-stoichiometric celsian synthesized by the thermal transformation of barium exchanged zeolite X. *J Solid State Chem* 2006;**179**: 1957–64.
19. Marocco A, Pansini M, Dell'Agli G, Esposito S. Parameters expediting the thermal conversion of Ba-exchanged zeolite A in monoclinic celsian. *Adv Mater Sci Eng* 2010;**vol. 2010**:8. doi:10.1155/2010/683429, Article ID 683429.
20. Marocco A, Esposito S, Dell'Agli G, Pansini M. Role of Na+ and Li+ in the thermal transformation of Ba-exchanged zeolite A in monoclinic celsian. *Solid State Sci* 2011;**13**:1143–51.
21. Andreola F, Romagnoli M, Siligardi C, Manfredini T, Ferone C, Pansini M. Densification and crystallization of Ba-exchanged zeolite A powders. *Ceram Int* 2008;**34**:543–9.
22. Cerri A, Langella M, Pansini P, Cappelletti. Methods for determination of cation exchange capacity for clinoptilolite-rich rocks of the Logudoro region in Northern Sardinia, Italy. *Clay Clay Miner* 2002;**50**: 127–35.
23. Breck DW. *Zeolite molecular sieves: structure, chemistry and use*. New York: Wiley; 1974.
24. Sherry HS, Walton HF. The ion-exchange properties of zeolites. II. Ion exchanged in the synthetic zeolite Linde 4A. *J Phys Chem* 1967;**71**:1457–65.
25. ASTM regulation C373-88. Standard test for water absorption, bulk density, apparent porosity and apparent specific gravity of fired whiteware products; 2006.
26. Hoghooghi B, McKittrick J, Helsel E, Lopez O. Microstructural development, densification, and hot pressing of celsian ceramics from ion-exchanged zeolite. *J Am Ceram Soc* 1998;**81**:845–52.

27. Fu YP, Chang CC, Lin CH, Chin TS. Solid-state synthesis of ceramics in the BaO–SrO–Al_2O_3–SiO_2 system. *Ceram Int* 2004;**30**:41–5.
28. Bernache-Assolant D, Montanaro L. La sinterizzazione di compatti di polveri – Parte II. *Ceramurgia* 1998;**28**:94–104.
29. Subramanian MA, Corbin DR, Farlee RD. X-ray and MAS NMR characterization of the thermal transformation of Li(Na)/1bY zeolite to lithium aluminosilicates. *Mater Res Bull* 1986;**21**:1525–32.
30. Chowdry UV, Corbin DR, Subramanian MA. Anorthite–cordierite based ceramics from zeolites US Patent 4,813,303; March 1989.
31. Subramanian MA, Corbin DR, Chowdry UV. Zeolites as precursors to alluminosilicate based ceramics for microelectronic packaging. *Adv Ceram* 1989;**26**:239–47.
32. Corbin DR, Parise JB, Chowdry UV, Subramanian MA. Designing zeolites as novel precursors to electronic ceramics. *Mater Res Symp Proc* 1991;**233**:213.
33. Baerlocher C, Meier WM, Olson DH. *Atlas of the zeolite framework types*. Amsterdam: Elsevier; 2001.